LOAD FREQUENCY CONTROL OF TWO-AREA POWER SYSTEM WITH A STAND ALONE MICROGRID BASED ON ADAPTIVE MODEL PREDICTIVE CONTROL

A. Anjaiah[1]

A. Mamatha, *Assistant Professor EEE, Tkr College of Engineering &Technology (Autonomous), India*

A. Anjaiah, *Assistant Professor EEE, Tkr College of Engineering &Technology (Autonomous), India*

K Arun kumar, *UG student, EEE, Tkr College of Engineering &Technology (Autonomous), India*

N Sharath Chandra, *UG student, EEE, Tkr College of Engineering &Technology (Autonomous), India*

S Shiva Kumar, *UG student, EEE, Tkr College of Engineering &Technology (Autonomous), India*

Y Naveen, *UG student, EEE, Tkr College of Engineering &Technology (Autonomous), India*

Abstract

This article suggests using adaptive model predictive control, or AMC, to manage the load frequency of a stand-alone microgrid connected to a two-area interconnected power system. In order to forecast the future output and control inputs for the microgrid frequency control, a generalized state-space model of a typical stand-alone microgrid with controllable and uncontrollable generating power sources is developed. The primary goal is to find solutions for frequency deviation issues related to load disturbance and changes in system characteristics Investigations are being conducted on how changes in system characteristics affect the effectiveness of frequency control in a stand-alone microgrid. For the various scenarios taken into consideration, the closed-loop response produced by the suggested AMPC has shown to be more responsive and flexible. Additionally, it is investigated how resilient AMPC is to changes in the system parameters. Furthermore, the effects of a few physical limitations on the power system's dynamic performance—such as the dead band (DB) for steam turbines, the reheat turbine (RT), the time delay (TD), and the generation rate constraint (GRC)—were examined. The simulation results of the suggested model showed that the suggested AMPC approach outperformed the MPC control technique and had strong dynamic response and robustness in addition to optimal performance.

Keywords— *Adaptive, load frequency control (LFC), microgrid, renewable, robustness and physical constraints.*

I. INTRODUCTION

Sustaining the intended quality and continuity of the electrical supply is one of the objectives of the power system utility [1]. As long as the generation and consumption of electrical energy are in balance, the power system is assumed to be in a state of continuous equilibrium. The primary goal of automatic generation control (AGC) in an interconnected power system is to lessen the variance in the transient response in the region frequency, tie-line power exchange. To offset the steady-state inaccuracy brought on by primary frequency regulation, AGC was created. For large-scale stability in multi-area power networks, frequency is an important stability requirement [2] As the penetration level of renewable distribution production increases, the load frequency control (LFC) problem of a multi-area linked power system with a stand-alone microgrid becomes more difficult due to the major challenges of unpredictability and uncertainty [2]. Therefore, the frequency controller needs to be carefully and

suitably developed in order to guarantee the stability of the standalone microgrid. More critically, more focus is needed on the load frequency control for microgrid operations in the distribution network, especially for the microgrid's off-grid remote operation. As a result, the microgrid's low inertia, converter-based, intermittent generation of distributed energy resources that are renewable present serious issues.

greater critically, greater focus is needed on the load frequency management for microgrid operations in the distribution network, especially for the microgrid's off-grid remote operation.

As a result, the microgrid's low inertia, intermittent, converter-based renewable distributed energy resource generation presents serious issues. Because of this, it necessitates the use of sophisticated control strategies to guarantee a steady supply to loads and further minimize the system's frequency deviation [3]. In autonomous microgrid operation, frequency and voltage regulation within designated nominal values is a crucial component for dependable system functioning and has gotten enough attention. The purpose of the battery energy storage system (BESS) in the standalone micro-grid (MG) system with secondary frequency control is to improve the performance of frequency control.

II. DYNAMIC SYSTEM MODELING FOR THE UNDER STUDY MICROGRID

An example of an integrated power system with two areas in Fig. 1, where control area 2 is made up of a thermal RT system, TD, DB, and GRC, and control area 1 is a multirenewable energy-based microgrid (PV generation system, fuel cell, wind turbine system, and battery). Furthermore, the governor's linearized models, thermal with RT, PV system, wind turbine system, fuel cell system, battery storage system, and UPFC connected, as well as the ac–dc tie line, were employed in the study's simulation of the transfer function model, as seen in Fig. 1. The control area 2 units' contributions to the nominal loading are determined by their respective regulatory parameters, R, and participation factor, Kt. Two control strategies are examined in this study to evaluate their control abilities in the reduction ofACE of the areas under control is almost zero. Therefore, it is essential to incorporate physical limitations in the dynamic model in order to gain a comprehensive understanding of the AGC problem. model of the system to offer a power system that is more useful. As a result, several of the generating units have certain crucial physical limits, such TD, GRC, and DB for the governor and steam turbines, and these nonlinear features have frequently been disregarded in some publications [29]. As a result, this article includes some physical limitations to make up for this flaw in the suggested model. Further more enhancing the power system's dynamic performance is the UPFC, a transmission system that belongs to the flexible alternating currents transmission systems (FACTS) family, which is used in series with a tie line.

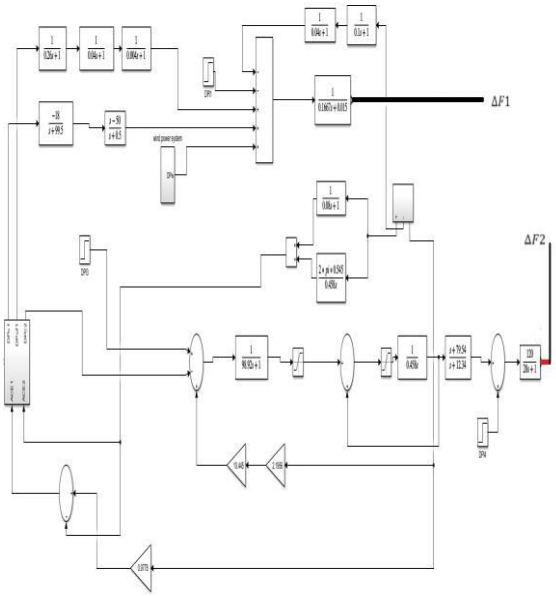

Fig. 1 Simulink Model of transfer function for an autonomous microgrid

based on two areas and multiple renewable energy sources

$$\Delta \dot{F}_1(t) = \frac{1}{2H}[\Delta P_{f\_filt1}(t) + \Delta P_{PV1}(t) + \Delta P_{W1}(t) - \Delta P_{bat1}(t) - \Delta P_{L1}(t) - D\Delta F_1(t) - \Delta P_4(t)]$$

$$\Delta \dot{F}_2(t) = \frac{K_{P1}}{T_{P1}}\Delta P_{tie}(t) - \frac{1}{T_{P2}}\Delta F_2(t) + \frac{K_{P2}}{T_{P2}}\Delta P_4(t) - \frac{K_{P2}}{T_{P2}}\Delta P_{L2}(t)$$

$$\Delta \dot{P}_1(t) = -a_1\Delta P_1(t) + K_1\Delta P_{C1}(t) \quad (3)$$

$$\Delta \dot{P}_{fC1}(t) = \frac{1}{T_{fC1}}[\Delta P_{Cf1}(t) - \Delta P_{fC1}(t)] \quad (4)$$

$$\Delta \dot{P}_{f\_inv1}(t) = \frac{1}{T_{inv1}}[\Delta P_{fC1}(t) - \Delta P_{f\_inv1}(t)] \quad (5)$$

$$\Delta \dot{P}_{f\_filt1}(t) = \frac{1}{T_{filt1}}[\Delta P_{f\_inv1}(t) - \Delta P_{f\_filt1}(t)] \quad (6)$$

$$\Delta \dot{P}_{bat1}(t) = \frac{1}{T_b}[\Delta F_1(t) - \Delta P_{bat1}(t)] \quad (7)$$

$$\Delta \dot{P}_{PV1}(t) = (b_1 - a_1)\Delta P_1(t) - C_1\Delta P_{PV1}(t) + K_1\Delta P_{C1}(t) \quad (8)$$

$$\Delta \dot{P}_2(t) = -\frac{R}{T_g}\Delta F_2(t) - \frac{1}{T_g}\Delta P_2(t) + \frac{1}{T_g}\Delta P_{C2}(t) + \frac{1}{T_g}\Delta P_{L3}(t) \quad (9)$$

$$\Delta \dot{P}_3(t) = \frac{1}{T_t}\Delta P_2(t) - \frac{1}{T_t}\Delta P_3(t) \quad (10)$$

$$\Delta \dot{P}_4(t) = \frac{K_r T_r}{T_t T_r}\Delta P_2(t) + \left(\frac{1}{T_r} - \frac{K_r T_r}{T_t T_r}\right)\Delta P_3(t) - \frac{1}{T_r}\Delta P_4(t) \quad (11)$$

$$ACE_1(t) = \Delta P_{tie}(t) = \frac{2\pi T_{12}(\Delta F_1(s) - \Delta F_2(s))}{s} \quad (12)$$

$$ACE_2(t) = -\Delta P_{tie}(t) + B\Delta F_2(t) \quad (13)$$

$$\Delta \dot{P}_{tie}(t) = \frac{1}{T_{UPFC1}}[2\pi T_{12}(\Delta P_{PV1}(t) + \Delta P_{filt1}(t) + \Delta P_{W1}(t) - \Delta P_{bat1}(t)) - \Delta P_{tie}(t) - \Delta F_2(t) - \Delta P_{L1}(t)] \quad (14)$$

where Ptie(t) is the overall tie-line power change in this system, P2(t), P3(t), and P4(t) are the PV power changes, and PPV1(t) is the PV power change.

the reheater, steam turbine, and governor power changes, in that order. The frequency variations of area 1 and area 2 are denoted by F1(t) and F2(t), respectively; the control actions of area 1 and area 2 are represented by PC1(t) and PC2(t), respectively; the load changes are denoted by PL1(t), PL2(t), and PL3(t); the frequency bias factor is represented by B; and the regulatory parameter is represented by R (Hz/p.u.MW). The nomenclature section contains a list of various parameters and their definitions.

III. MPC Controller Architecture Based on Adaptive Mode To apply MPC based on adaptive in this study

For the control system's nominal operating conditions, we created a traditional model predictive controller. Next, over the course of the prediction horizon, the plant models and the nominal conditions that the MPC controller uses are updated [32]. In addition, an AMPC algorithm is employed to automatically adjust the weights of various targets based on the system's current condition. The basic idea of the suggested method is to create a system dynamic Thus, by minimizing the weighted sum of squares, a rolling optimization of the control signal is implemented based on the cost function.

square future control values and anticipated mistakes [31], [33]. Theoretically, the expanded discrete-time state-space model is reformed as per (17) and (18) [25] by establishing an extended state vector Z(k) = (x(k)y(k − 1))T.

$$Z(k+1) = GZ(k) + H\Delta(k) + H_1\Delta u_1(k) \quad (20.1)$$

$$y(k) = C_z Z(k) + D\Delta u(k) \quad (20.2)$$

$$G = \begin{pmatrix} A_d & 0_{N_x \times N_y} \\ C & E_{N_y} \end{pmatrix}_{(N_x+N_y)\times(N_x+N_y)}$$

$$H = \begin{pmatrix} B_d \\ 0_{N_y \times N_u} \end{pmatrix}_{(N_x+N_y)\times N_u}$$

$$H_1 = \begin{pmatrix} B_{1d} \\ 0_{N_y \times N_{u1}} \end{pmatrix}_{(N_x+N_y)\times N_{u1}}$$

$$C_z = \begin{pmatrix} C & E_{N_y} \end{pmatrix}_{N_y \times N_x + N_y}$$

and u1(t), in that order. The following is an estimate of the predicted output value y(k + p|k) at the kth sampling time: where M denotes the control horizon and P the prediction horizon. The following equation [34] is used to estimate the predictive output vector YP (k):

$$= C_z G^p Z(k) + \sum_{j=1}^{r} C_z G^{p-j} H \Delta u(k+j-1)$$

$$+ \sum_{j=1}^{p} C_z G^{p-j} H_1 \Delta u_1(k+j-1),\ p = 1,2\ldots,p \quad (21)$$

Furthermore, a conventional constrained MPC problem is used to design the optimal LFC problem of a multi-area power system with the penetration of renewable energy sources [31].

$$Y_P(k) = \emptyset Z(k) + \varphi \Delta U(k) + \varphi_1 \Delta U_1(k).$$

Furthermore, a conventional constrained MPC problem is used to design the optimal LFC problem of a multi-area power system with the penetration of renewable energy sources [31].

$$\text{iin } J(k) = \min\{(Y_P(k) - Y_r(k))^T Q(Y_P(k) - Y_r(k)) + (\Delta U(k))^T R(\Delta U(k))\}. \quad (23)$$

The control signal's limitations, outputs, and control signal change are expressed as follows, depending on the operation's system performance [34].

$$\text{s.t.} \quad (24)$$

$$u_{\min} \le u(k) \le u_{\max} \quad (24.1)$$

$$\Delta u_{\min} \le \Delta u(k) \le \Delta u_{\max} \quad (24.2)$$

$$y_{\min} \le y(k) \le y_{\max} \quad (24.3)$$

where umin and umax are the lower and upper bounds, and Q and R are the weighting vectors to balance the performance of squared anticipated errors and squared future control values.

ymin and ymax are the lower and upper bounds, respectively, of the increment of the control signal vector <= u(k).
the system's output, which is y(k). To find the values of Q and R, similar empirical criteria and trial and error methods can be used. The control signal's ideal sequence
When the constraints indicated in (24) are taken into account, the solution of equation (23) provides over the horizon Nc. The control law u(k) is obtained by the following equations in accordance with the gradient descent approach, that is, (d J (k)/U(k)) = 0. [31]

$$\Delta U(k) = (\varphi^T Q \varphi + R)^{-1} \varphi^T Q(Y_r(k) - \emptyset Z(k) - \varphi_1 \Delta U_1(k)) \quad (25)$$

$$\Delta u(k) = \left(E_{N_u}\ 0_{N_u \times (P-1)}\right) \Delta U(k) \quad (26)$$

$$u(k) = \Delta u(k) + \Delta u(k-1). \quad (27)$$

(AMPC) for the LFC problem of a multi-area linked power system using renewable energy sources. based on the analysis presented above. Additionally, Fig. 3 displays the flowchart of the suggested control strategy used in this investigation.

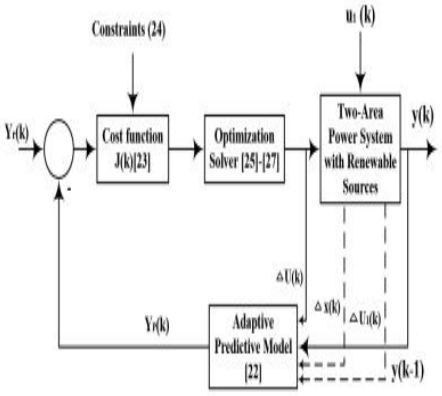

Fig.2 Block schematic of an AMPC control strategy for the investigated optimal LFC problem

IV. UPFC MODELING USED IN THE SUGGESTED SYSTEM MODEL

The last ten years have seen a steady and quick advancement in power electronics, which has made FACTS a viable idea for power system applications. Therefore, power flow in long transmission lines may be more flexibly managed with the implementation of FACTS technology.
One of the most adaptable devices in the FACTS family, the UPFC can control power flow in the transmission line, reduce oscillation

in the system, improve transient stability, and sustain voltage. Because the two-area power system with a UPFC is connected in series with a tie line, the tie-line power is guaranteed to be dampened by oscillations [1].

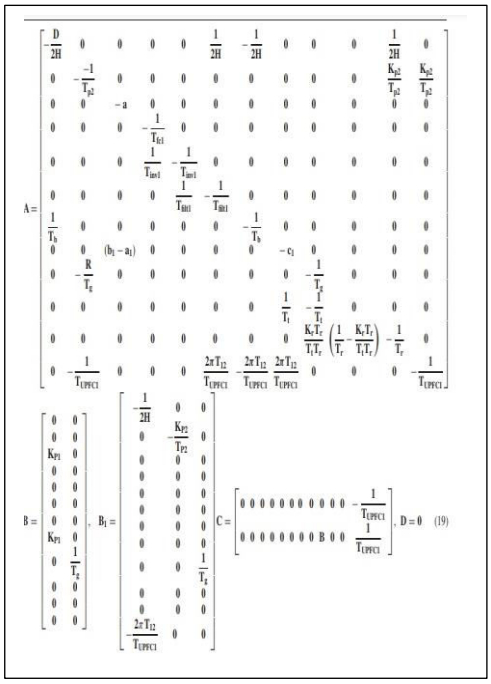

V. SIMULATION RESULTS AND DISCUSSIONS

The simulation results and explanations of several situations of the LFC problem in a two-area stand-alone microgrid with renewable sources are presented in this part. Thus, in order to illustrate the efficacy of the suggested AMPC scheme, we examined several scenarios, including changes to the system. parameters, load, and generation. Simulink/MATLAB is used to simulate the two-area multisource power network with renewable energy sources that is depicted in Figure 1.

Because power systems are becoming more complicated in a deregulated environment, communication delays provide a significant difficulty in the investigation of LFC problems. These physical limitations are part of the system model to make the analysis of the suggested model more realistic.

The following are the parameters of the simulation system:

$$T_{12} = 0.545 \text{ p.u}, T_p = 20 \text{ s}, T_t = 0.3 \text{s}, T_r = 10 \text{ s}, T_g = 0.08 \text{ s}, K_{P2} = 120 \text{ Hz/p} \cdot \text{uMW}, K_g = K_t = 1 \text{ Hz/p} \cdot \text{uMW}, K_r = 1 \text{ Hz/p} \cdot \text{uMW}, B = 0.08 \text{ p} \cdot \text{uMW/Hz}, R = 0.4 \text{ Hz/p} \cdot \text{uMW}, K_{P1} = 0.33 \text{ p.uMW}, a_1 = 99.5, c_1 = 0.5, b_1 = -50, K_{P1} = -18, 2H = 0.1667 \text{ s}, D = 0.015 \text{ p.u} \cdot \text{MW/Hz}, T_{fc} = 0.26 \text{ s}, T_{inv} = 0.04 \text{ s}, T_{filt} = 0.004 \text{ s}, \text{and } T_b = 0.1 \text{ s}.$$

The schematic depiction of the system under investigation is displayed in Fig. 3. Comparison based on robustness, optimum performance, robust dynamic response, and the superiority of the

Examined is the suggested AMPC approach in relation to the MPC control technique. In order to evaluate the resilience and dynamic reactivity of the AMPC-based secondary frequency control, a number of scenarios are run while taking the system uncertainties into account. Additionally, by looking at the MG system, the dynamic reactions of both controllers are evaluated under load change and wind power changes.

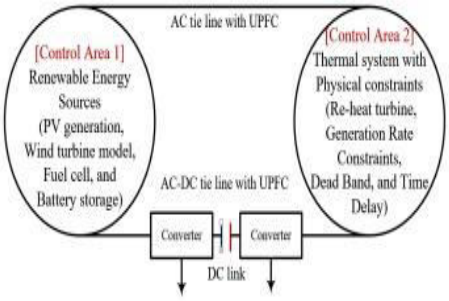

Fig.3 Isolated microgrid with two areas of renewable sources and UPFC

Table 1 PROPOSED CONTROL SCHEME AND ADDITIONAL EVOLUTIONARY ALGORITHMS FOR PARAMETERS

Algorithms	Parameters Setting
AMPC	Prediction horizon, $P = 10$, control horizon, $M = 5$, weights on manipulated variables = 0.01, weights on manipulated variables rate = 0.02, weights on the output signals = 1.2, sampling interval = 0.0002 s, Max. control action = 0.2 pu, Min. control action = 0.2 pu, Max. Frequency deviation= 1 pu, Min. frequency deviation= 1 pu, weight vectors, $Q = E_{P\times P}$, $R = 0.01E_{M\times M}$.
Conventional MPC	Prediction horizon, $P = 10$, control horizon, $M = 5$, weight vectors, $Q = E_{P\times P}$, $R = 0.01E_{M\times M}$.

Table 1 shows the various parameters setting of AMPC and MPC control techniques.

Case 1a and 1b : Variation in Step Load and Dynamic System Reaction

In this instance, the microgrid's dynamic system reaction the load is assessed using series step adjustments. The load modifications are applied with a rise in PL value. As seen in Fig. 4(a), the load connects to the stand-alone microgrid system at 5 s with an amount of 0.02 p.u. (2% step increase in load with ac tie line), which causes the frequency to decrease. Furthermore, the ESS's secondary frequency control, which produces more active power, allows the microgrid frequency to return to its nominal value.

Fig. 4(b) makes it clear that the AMPC control approach produced better control performance for the microgrid frequency than the MPC control technique. When AMPC is used, the frequency response is improved and quicker, and the overshoot is much lower as compared to the MPC method. When the controller is not included, the thermal system's dynamic transient response and optimal controller parameter values are impacted by physical restrictions (nonlinear characteristics), which leads to increased oscillations.

The integral of time multiplied square error, the integral of time multiplied absolute value of the error, the integral of the absolute value of the error, and the integral of square error are the performance indices (Criteria) used in this study.

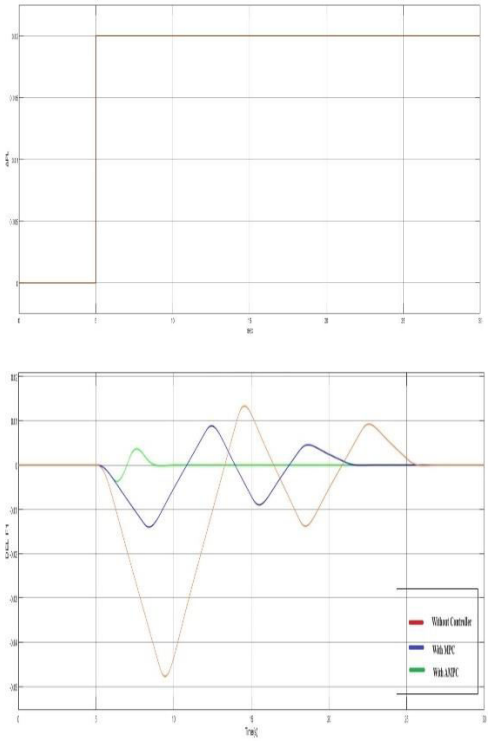

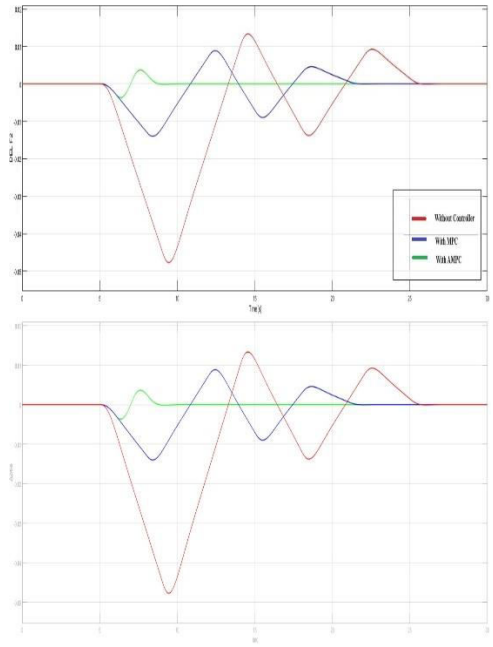

Fig.4 System's dynamic reaction to a 2% step increase in load using an ac tie-line: (a) Disturbance in load. (b) The frequency deviation of Area 1. (c) Frequency variation in Area 2. (c) Variation in tie-line power

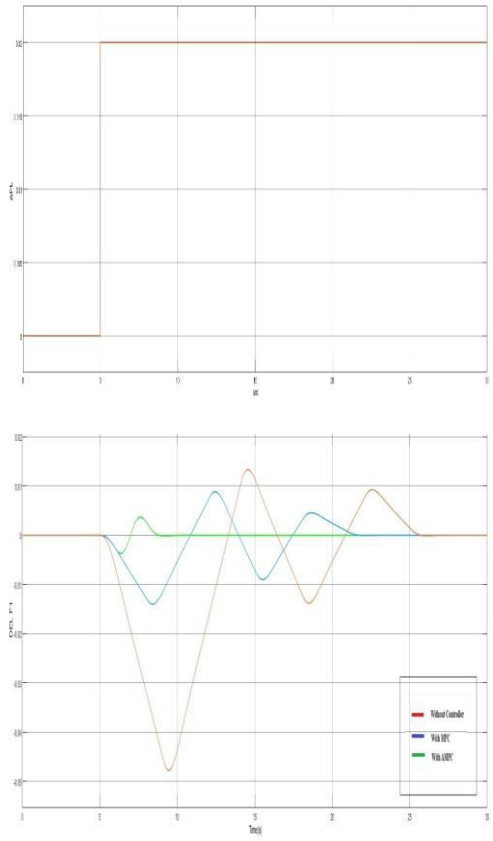

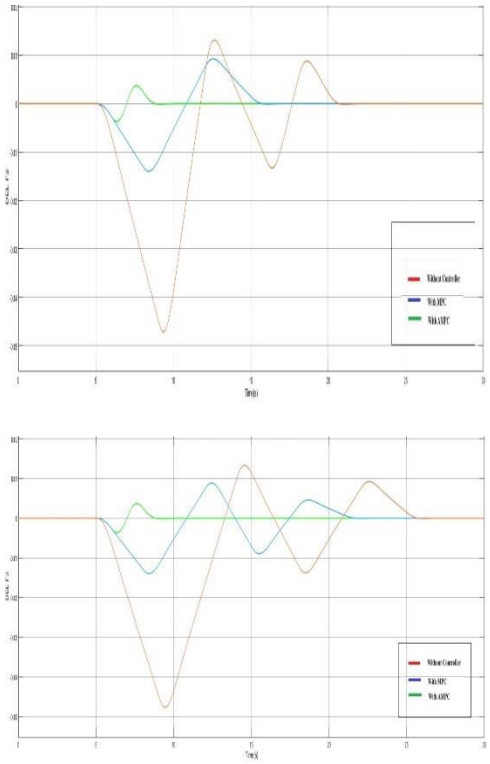

Fig.5 System's dynamic reaction with an ac-dc tie-line to a 2% step increase in load: (a) Disturbance in load (b) The frequency deviation of Area 1. (c) The frequency deviation of Area 2. (d) Power variation of the tie-line.

Table 2 A COMPARISON OF THE CONTROL TECHNIQUES' SYSTEM PERFORMANCE USING THE PERFORMANCE INDICES IN CASE 1-A

Algorithms / Performance indices	AMPC	MPC	WITHOUT CONTROLLER
ITAE	7.35	19.28	134.39
ITSE	0.44	0.96	9.87
IAE	9.58	14.13	39.52
ISE	0.32	0.98	8.65

Table 3 A COMPARISON OF THE CONTROL TECHNIQUES' SYSTEM PERFORMANCE USING THE PERFORMANCE INDICES IN CASE 1-B

Algorithms / Performance indices	AMPC	MPC	WITHOUT CONTROLLER
ITAE	9.15	21.45	142.45
ITSE	0.65	0.96	9.53
IAE	11.68	17.95	44.05
ISE	0.58	0.95	11.76

CONCLUSION

This research proposes an adaptive AMPC approach for load frequency control in a two-area linked power system that leverages renewable energy sources in order to achieve optimal system performance. Both the ac tie line and the ac–dc tie line are treated with the UPFC. The effect of parametric uncertainty on the performance of the control techniques has been investigated in this study. The acquired findings unequivocally show that compared to the traditional MPC control approach, the AMPC control technique is more resilient against system uncertainties. Furthermore, AMPC-based microgrid frequency regulation responds quicker than MPC-based frequency management.
Additionally, because renewable energy sources (solar and wind power) are widely used, the AMPC-based frequency management maintains the microgrid frequency within the allowed frequency deviation range. The recommended AMPC controller outperformed the conventional MPC in terms of performance indices and dynamic response performance, according to the examination of four scenarios. The recommended controller further shown its superiority even in the face of tangible limitations like DB, TD, and GRC.The impact of the UPFC linked in series with the tie line on the system's dynamic performance was examined. As a result, there was a noticeable improvement in both the performance indices and the dynamic reaction performance.

REFERENCES

[1] P. C. Pradhan, R. K. Sahu, and S. Panda, “Firefly algorithm optimized fuzzy PID controller for AGC of multi-area multi-source power systems with UPFC and SMES,” Eng. Sci. Technol., Int. J., vol. 19, no. 1, pp. 338–354, Mar. 2016.
[2] S. K. Pandey, S. R. Mohanty, and N. Kishor, “A literature survey on load–frequency control for conventional and distribution generation power systems,” Renew. Sustain. Energy Rev., vol. 25, pp. 318–334, Sep. 2013.
[3] D. E. Olivares et al., “Trends in microgrid control,” IEEE Trans. Smart Grid, vol. 5, no. 4, pp. 1905–1919, Jul. 2014.
[4] J. M. Guerrero, J. C. Vasquez, J. Matas, L. García de Vicuna, and M. Castilla, “Hierarchical control of droop-controlled AC and DC Microgrids—A general approach toward standardization,” IEEE Trans. Ind. Electron., vol. 58, no. 1, pp. 158–172, Jan. 2011.
[5] S. Panda and N. K. Yegireddy, “Automatic generation control of multiarea power system using multi-objective non-dominated sorting genetic algorithm-II,” Int. J. Electr. Power Energy Syst., vol. 53, pp. 54–63, Dec. 2013.
[6] A. M. Ersdal, L. Imsland, and K. Uhlen, “Model predictive Loadfrequency control,” IEEE Trans. Power Syst., vol. 31, no. 1, pp. 777–785, Jan. 2016.
[7] Y. Mi, Y. Fu, C. Wang, and P. Wang, “Decentralized sliding mode load frequency control for multi-area power systems,” IEEE Trans. Power

Syst., vol. 28, no. 4, pp. 4301–4309, Nov. 2013.

[8] S. Saxena and Y. V. Hote, "Stabilization of perturbed system via IMC: An application to load frequency control," Control Eng. Pract., vol. 64, pp. 61–73, Jul. 2017.

[9] K. Sabahi, M. Teshnehlab, and M. A. Shoorhedeli, "Recurrent fuzzy neural network by using feedback error learning approaches for LFC in interconnected power system," Energy Convers. Manage., vol. 50, no. 4, pp. 938–946, Apr. 2009.

[10] N. El Yakine Kouba, M. Menaa, M. Hasni, and M. Boudour, "Optimal control of frequency and voltage variations using PID controller based on particle swarm optimization," in Proc. 4th Int. Conf. Syst. Control (ICSC), Apr. 2015, pp. 424–429